RSC Advances

PAPER

View Article Online
View Journal | View Issue

Cite this: *RSC Adv.*, 2019, **9**, 10195

$Y_3Al_5O_{12}$:Ce nanoparticles made by ionic-liquid-assisted particle formation and LiCl-matrix-treated crystallization

Hannah F. Gaiser, Ana Kuzmanoski and Claus Feldmann *

Received 28th February 2019
Accepted 25th March 2019

DOI: 10.1039/c9ra01537j

rsc.li/rsc-advances

$Y_3Al_5O_{12}:Ce^{3+}$ (YAG:Ce) nanoparticles were prepared by a two-step approach including ionic-liquid-assisted particle formation and LiCl-matrix-treated crystallization. Subsequent to particle formation in $[MeBu_3N][N(SO_2CF_3)_2]$ as the ionic liquid ($MeBu_3N$: tributylmethylammonium; $N(SO_2CF_3)_2$: bis(trifluoromethanesulfonyl)imide), the as-obtained amorphous precursor nanoparticles were crystallized in a LiCl matrix (600 °C, 1 h). The resulting YAG:Ce nanoparticles are well crystallized and exhibit a diameter of about 40 nm. They show bulk-like luminescence and a quantum yield of 51(±3)%. The selected Y : Al ratio and temperature profile turned out to be optimal for the synthesis strategy in terms of particle size and luminescence properties although minor amounts of CeO_2 remained. The YAG:Ce nanoparticles can be easily redispersed in the liquid phase and embedded in polymers such as polyester. The course of the reaction and the properties of the nanoparticles are characterized by electron microscopy, dynamic light scattering, infrared spectroscopy, X-ray powder diffraction, and fluorescence spectroscopy.

Introduction

Cerium-doped yttrium aluminium garnet ($Y_3Al_5O_{12}:Ce^{3+}$, YAG:Ce) is one of the most efficient luminescent materials and is applied, for instance, in phosphor-converted white-light emitting diodes (pc-WLEDs).[1] Herein, YAG:Ce converts part of the blue light emitted by the (Ga,In)N-semiconductor chip into yellow emission, which – upon additive colour mixing – results in white light emission. Among a great number of known luminescent materials, YAG:Ce still represents one of the most efficient inorganic materials with a quantum yield of 80–90%.[2] Besides efficient luminescence processes, the excellent performance of bulk-YAG:Ce originates from the high lattice energy, the isotropy of cubic lattice, a low defect concentration and low-energy lattice vibrations, which, together, result in minimal non-emissive loss processes.[1–3]

The formation of YAG:Ce nanoparticles – in contrast to the bulk-phase – is a challenge. On the one hand, crystallization and removal of water and hydroxides at low temperatures (<500 °C) are difficult and often lead to highly defective YAG:Ce with quantum yields ≤ 20%. Post-sintering of the as-prepared YAG:Ce nanoparticles, on the other hand, foils the efforts of low-temperature particle formation and causes uncontrolled particle growth and agglomeration. Dispersible, nanosized (≤100 nm) and efficient YAG:Ce nanoparticles, however, are prerequisite to facile liquid-phase deposition, printing of thin films, or an incorporation into polymers.[1]

Nano- and micron-sized YAG:Ce was typically prepared at high temperature (800–1500 °C) *via* solid-state synthesis including molten-salts,[4] Pechini-type, flame-, plasma- or microwave-driven combustions,[5] spray pyrolysis or sintering in silica matrices.[6] Liquid-phase approaches comprise sol–gel,[7] polyol,[8] emulsion synthesis,[9] or co-precipitation processes.[10] The as-prepared, defective nanoparticles most often require post-synthesis calcination (1000–1200 °C) to adjust efficient luminescence processes. The highest quantum yields of dispersible YAG:Ce nanoparticles (∅ ≤ 100 nm) were yet reported with 50–60%.[6b,9a,11] These nanoparticles were either obtained by high-temperature sintering (≥1000 °C),[9a] calcination in difficult-to-remove SiO_2 matrices,[6] or by solvothermal synthesis at elevated pressure (70 bar),[11] which typically results in significant agglomeration and comparably broad size distributions.

Aiming at crystalline and dispersible YAG:Ce nanoparticles, we here suggest a novel two-step approach (Fig. 1). In a first step, amorphous precursor nanoparticles were obtained with optimal conditions of particle formation in ionic liquids (ILs). As a second step, the as-prepared, amorphous precursor nanoparticles were crystallized in a LiCl matrix at 600 °C. The resulting crystalline YAG:Ce nanoparticles were examined in detail in regard of particle size, dispersibility, chemical composition and luminescence properties.

Institut für Anorganische Chemie, Karlsruhe Institute of Technology (KIT), Engesserstraße 15, D-76131 Karlsruhe, Germany. E-mail: claus.feldmann@kit.edu; Tel: +49-721-60842855

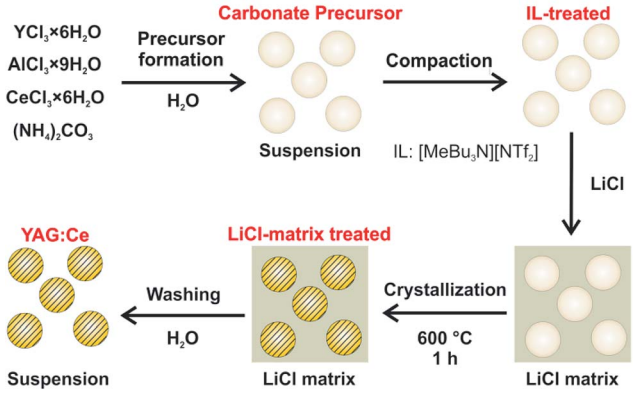

Fig. 1 Scheme illustrating the two-step synthesis of dispersible YAG:Ce nanoparticles, including IL-assisted particle formation and LiCl-matrix-treated crystallization.

Experimental

Synthesis

Starting materials. $YCl_3 \cdot 6H_2O$ (Alfa Aesar, 99.9%), $AlCl_3 \cdot 9H_2O$ (Riedel de Haen, 99.9%), $CeCl_3 \cdot 7H_2O$ (Aldrich, 99.9%), $(NH_4)_2CO_3$ (VWR, 99.9%), and LiCl (VWR, 99.5%) were used as supplied. The synthesis of the ionic liquid $[MeBu_3N][N(SO_2CF_3)_2]$ was performed based on a metathesis reaction with tributylmethylammonium chloride ($[N(CH_3)(C_4H_9)_3]Cl$) and lithium bis(trifluoromethane sulfonyl)imide ($Li[N(SO_2CF_3)_2]$) following a procedure given elsewhere.[12]

Ionic-liquid (IL) assisted particle formation. In a first step, the formation of precursor nanoparticles was performed in ionic liquids. To this concern, 432 mg (4.5 mmol) of $(NH_4)_2CO_3$ were dissolved in 50 mL of water. Thereafter, 455 mg (1.5 mmol) of $YCl_3 \cdot 6H_2O$, 603 mg (2.5 mmol) of $AlCl_3 \cdot 9H_2O$ and 39 mg (0.105 mmol) of $CeCl_3 \cdot 7H_2O$ were dissolved in 5 mL of water and injected to the $(NH_4)_2CO_3$ solution with vigorous stirring, which instantaneously results in the nucleation of colourless precipitate. Few drops of diluted, aqueous NH_3 were added to adjust a pH > 8. After 15 min, the obtained solid was centrifuged and washed with water. Thereafter, the colorless was dispersed in 20 mL of $[MeBu_3N][N(SO_2CF_3)_2]$ as the IL. The resulting suspension was heated in a microwave oven (MLS rotaprep) to 200 °C within 60 seconds and kept at this temperature for 60 minutes. After cooling, the resulting precursor nanoparticles were diluted and washed with ethanol.

LiCl-matrix treatment. In a second step, the collected precursor nanoparticles were dried in air in a drying oven (60 °C). For crystallization, the precursor nanoparticles were ground with 10-fold excess of solid LiCl and sintered thereafter for 1 h at 600 °C in a tube oven. Finally, LiCl was removed by dispersion/centrifugation of the YAG:Ce nanoparticles in water, which was performed twice.

YAG:Ce in polyester. To embed YAG:Ce in polyester, in a first step, 25 mg of LiCl-matrix-treated nanoparticles were resuspended in 10 mL of ethylene glycol. Thereafter, 4.5 g of citric acid were added to the suspension and dissolved with vigorous stirring. Finally, the dispersion was heated to 150 °C and kept at this temperature for 5 minutes to initiate and complete the polymerization. After natural cooling to room temperature, a soft, slightly yellowish and water-insoluble polyester resin was produced.

Analytical methods

Scanning electron microscopy (SEM). SEM was conducted on a Zeiss Supra 40 VP, using an acceleration voltage of 4 kV and a working distance of 4 mm. SEM samples were prepared by evaporation of ethanolic suspensions of the respective nanoparticles. The mean particle diameter was calculated by statistical evaluation of at least 500 particles.

X-ray powder diffraction (XRD). XRD was performed with a Stoe STADI-MP diffractometer operating with Ge-monochromatized Cu-Kα-radiation (λ = 1.54178 Å) and Debye–Scherrer geometry. The nanoparticle samples were fixed between Scotch tape and acetate paper and measured between −69° and +69° of two-theta.

Dynamic light scattering (DLS). DLS was used to determine the hydrodynamic diameter of the nanoparticles in suspension. Studies were conducted at room temperature in glass or polystyrene cuvettes applying a Nanosizer ZS (Malvern Instruments, United Kingdom).

Fourier-transformed infrared spectroscopy (FT-IR). FT-IR was performed on a Bruker Vertex 70. Samples were prepared by pestling of 1 mg of the respective nanoparticles with 300 mg of dried KBr in a glove box.

Photoluminescence spectroscopy (PL). PL was conducted with a Horiba Jobin Yvon Spex Fluorolog 3 (Horiba Jobin Yvon, France) equipped with a 450 W Xe-lamp and double grating excitation and emission monochromator. The determination of the quantum yield was performed as reported by Friend.[13] First of all, the diffuse reflection of the nanoparticulate powder sample was determined under excitation conditions (maximum of absorption at λ_{exc} = 554 nm). Thereafter, the emission was measured at this excitation wavelength. Integration over the reflected and emitted photons by use of the Ulbricht sphere results in the absolute quantum yield. All measurements were referenced to an empty sample holder. Corrections were made regarding the spectral power of the excitation source, the reflection behavior of the Ulbricht sphere, and sensitivity of the detector. To this concern, the FluorEssence Software Version 3.5.8.63 from Horiba Yvon Jobin GmbH was used.

Results and discussion

Ionic-liquid assisted particle formation

The here proposed two-step approach intends to separate particle formation and crystallization in order to optimize both independently (Fig. 1). Controlling particle size and particle agglomeration is of course essential in both steps of the reaction. In this regard, $Y(NO_3)_3 \cdot 6H_2O$, $Al(NO_3)_3 \cdot 9H_2O$, $Ce(NO_3)_3 \cdot 6H_2O$ and $(NH_4)_2CO_3$ were used as the starting materials and mixed in water to obtain a colourless, fluffy carbonate precursor. Fourier-transform infrared spectroscopy (FT-IR), as expected, indicates the characteristic carbonate-related vibrations (ν(C=O): 1600–1400, ν(C–O): 1100–

1000 cm^{-1}, Fig. 2). Due to the aqueous treatment, moreover, a broad vibration related to water is visible (ν(O–H): 3700–3000). Energy-dispersive X-ray (EDX) analysis, finally, already indicates a Ce : Y : Al ratio of 0.04 : 0.75 : 1 with excessive Y in relation to the intended ratio in $Y_3Al_5O_{12}$:Ce (5 mol%) of 0.03 : 0.57 : 1, which was naturally also the ratio introduced with the starting materials.

The amorphous and colourless carbonate precursor, thereafter, was dispersed in $[MeBu_3N][N(SO_2CF_3)_2]$ as the IL and rapidly heated in a microwave oven to 200 °C (Fig. 1). After ethanol-driven removal of the IL, FT-IR still shows the presence of the carbonate precursor (ν(C=O): 1600–1400, ν(C–O): 1200–1000 cm^{-1}) and water (ν(O–H): 3700–3000) in addition to surface-adhered IL (fingerprint: 1400–1100, Fig. 2). The latter finding is validated when comparing to the FT-IR spectra of the pure IL. Moreover, it is to be noted that the carbonate precursor is still amorphous and colourless subsequent to the IL treatment and does not show any specific Bragg peak (Fig. 3a and b). EDX analysis confirms the Y-rich composition and a Ce : Y : Al ratio of 0.04 : 0.75 : 1 as already determined for the carbonate precursor (0.04 : 0.71 : 1).

The IL treatment results in a compaction of the fluffy carbonate precursor and the formation of well-defined nanoparticles. Such IL-assisted treatment was already reported as promising for particle compaction and particle shaping,[14] which can be related to the high boiling point and the weakly coordinating properties of ILs.[15] In this regard, scanning electron microscopy (SEM) shows uniform, non-agglomerated nanoparticles with a mean diameter of 33 ± 6 nm (Fig. 5a). This diameter matches well with dynamic light scattering (DLS) indicating a mean hydrodynamic diameter of 39 ± 7 nm in diethylene glycol (DEG) (Fig. 5a). DEG was selected as dispersant due to its stabilizing properties in order to avoid agglomeration during the redispersion process.[16] Moreover, such dispersions in polyols are relevant as they offer the opportunity of direct polymerization and nanoparticle incorporation in polyesters.[17]

LiCl-matrix-treated crystallization

Subsequent to the IL-assisted particle formation, the carbonate precursor nanoparticles were mixed and pesteled with LiCl in a ratio of 1 : 10. As a result, the nanoparticles were separated from each other and embedded in a LiCl matrix (Fig. 1). This solid mixture was then heated to 600 °C in a tube oven for 60 minutes in order to decompose the carbonate precursor and to crystallize the YAG phase. Moreover, the separation of the nanoparticles in the LiCl matrix allows avoiding particle growth and particle agglomeration. Subsequent to this LiCl-matrix treatment, LiCl was removed by simple rinsing with demineralized water which was performed twice. After each washing step, the nanoparticles were collected by centrifugation. The characteristic intense yellow colour of obtained powder samples already indicates successful crystallization of YAG:Ce (Fig. 3c).

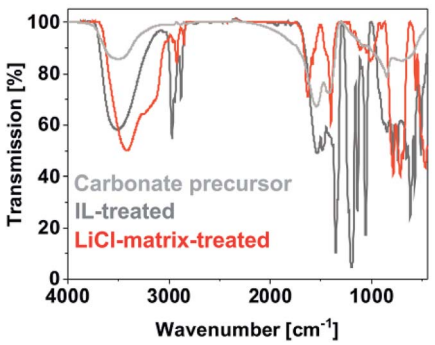

Fig. 2 Course of the reaction analysed by FT-IR spectroscopy with spectra of the carbonate precursor nanoparticles, IL-treated precursor nanoparticles, and LiCl-matrix-treated YAG:Ce nanoparticles.

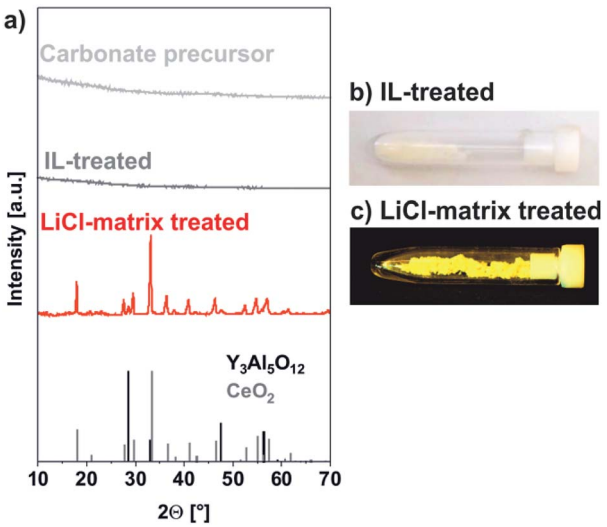

Fig. 3 Course of the reaction analysed by X-ray powder diffraction with (a) XRD patterns of carbonate precursor nanoparticles, IL-treated precursor nanoparticles, LiCl-matrix-treated YAG:Ce nanoparticles (references: $Y_3Al_5O_{12}$ – ICDD no. 088-2048/black line pattern; CeO_2 – ICDD no. 081-0792/grey line pattern); (b and c) photos of IL-treated and LiCl-matrix treated powder samples in daylight.

This LiCl-matrix treatment indeed results in an effective decarboxylation of the precursor nanoparticles as indicated by significantly reduced intensities of the ν(C=O), and ν(C–O) vibrations (Fig. 2). In fact, only lattice vibrations (ν(Al–O): 900–500 cm^{-1}) and vibrations of surface-adhered water stemming from the washing procedure remain (ν(O–H): 3700–3100 cm^{-1}; δ(O–H): 1620, 1450 cm^{-1}).

In contrast to the amorphous carbonate precursor obtained after IL-treatment, the LiCl-matrix-treated nanoparticles turned out as highly crystalline (Fig. 3a). Thus, the observed Bragg peaks are well in accordance with the garnet phase. Just a weak Bragg peak at 28.5° of 2-theta points to the presence of CeO_2 (Fig. 4). Here, it must be noticed that all efforts to adjust the ratio of the starting materials either resulted in low amounts of either CeO_2 (Y : Al ≤ 0.6 : 1) or $YAlO_3$:Ce (Y : Al > 0.6 : 1) as a side phase. Most interestingly, no Bragg peaks of LiCl were observed, indicating that the washing procedure guarantees complete removal of all LiCl (Fig. 3a and 4). Even flame colouring with the as-obtained YAG:Ce nanoparticles did not result in any characteristic red and orange emission lines of lithium.[18] Finally, a slight shift to smaller two-theta values in comparison

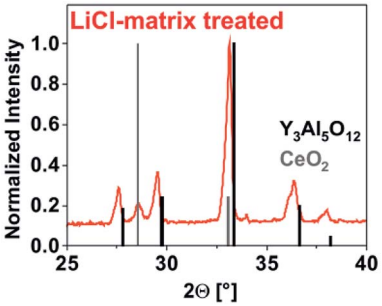

Fig. 4 Enlarged view of the XRD pattern to indicate minor amount of CeO_2 (references: $Y_3Al_5O_{12}$ – ICDD no. 088-2048 (black line pattern); CeO_2 – ICDD no. 081-0792 (grey line pattern)).

to bulk-YAG points to the incorporation of the larger Ce^{3+} (103 pm) on lattice sites of Y^{3+} (89 pm), resulting in increased lattice distance (Fig. 4).

The particle size of the LiCl-matrix-treated YAG:Ce nanoparticles was again verified by SEM (Fig. 5b). Accordingly, a mean diameter of 41 ± 9 nm was observed, which is only slightly larger as compared to the IL-treated carbonate precursor nanoparticles (33 ± 6 nm). Although crystallized at 600 °C in the LiCl-matrix, the YAG:Ce nanoparticles are still spherical and non-agglomerated, which indicates the feasibility of the LiCl-matrix sintering. After redispersion in DEG, the YAG:Ce nanoparticles exhibit a larger hydrodynamic diameter of 93 ± 15 nm (Fig. 5b) as compared to the IL-treated precursor nanoparticles (39 ± 7 nm), which points to at least some agglomeration. Nevertheless, the YAG:Ce nanoparticles turned out as redispersible and still have a mean diameter < 100 nm.

In addition to the particle size, the mean crystallite diameter was deduced from the width of the Bragg peaks *via* the Scherer formalism and resulted in 25–30 nm. Within the significance of the measurement, this value is in agreement with the diameter stemming from SEM and points to the single-crystalline nature of the YAG:Ce nanoparticles. Finally, EDX analysis confirms a Ce : Y : Al ratio of 0.04 : 0.75 : 1 with certain excess of Y in relation to the intended ratio in $Y_3Al_5O_{12}$:Ce (5 mol%) with 0.03 : 0.57 : 1. Whereas this ratio is constant for the whole sequence of synthesis, it is different from the ratio introduced with the starting materials ((Y + Ce) : Al = 0.6 : 1). The lack of Al^{3+} can be ascribed to its small size and its higher solubility in the liquid phase as compared to Y^{3+}. Any decrease of the Y^{3+} content (*i.e.*, a ratio Y : Al < 0.6 : 1), however, resulted in significant amounts of CeO_2 as a side phase. Such behaviour is often observed for low-temperature synthesis, where the effect of the different radii of the cations is more significant than for conventional solid-state synthesis at high temperatures (800–1500 °C).[4–10] Taken together, the here applied Y : Al ratio and temperature treatment turned out as optimum for the presented synthesis strategy in terms of particle size and luminescence properties.

Luminescence characterization

The luminescence properties of the LiCl-matrix-treated YAG:Ce nanoparticles were finally examined by fluorescence spectroscopy. Excitation spectra show weak absorption due to 4f → 5d transition on Ce^{3+} (330–360 nm, maximum at 342 nm) and strong absorption at 410–520 nm, peaking at 454 nm, related to O^{2-} → Ce^{3+} charge-transfer transition (Fig. 6a). Emission spectra indicate intense yellow light emission by 5d → 4f transition on Ce^{3+} at 500–680 nm with its maximum at 567 nm (Fig. 6b).[1,3] With these features, excitation and emission of the

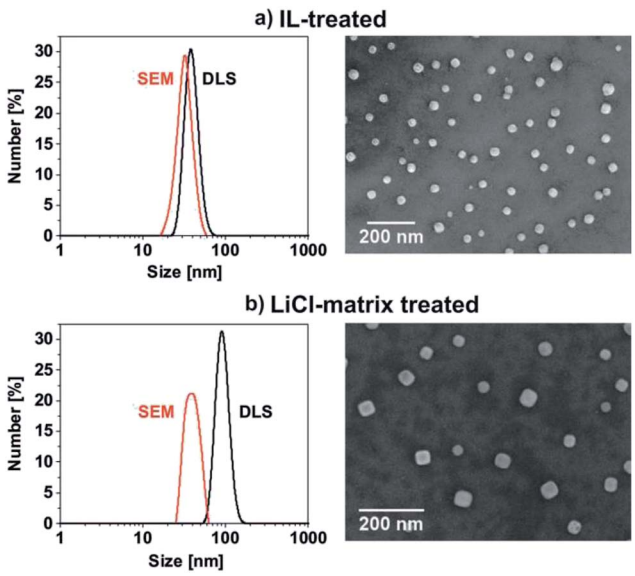

Fig. 5 Size and size distribution of (a) the carbonate precursor nanoparticles after IL-treatment (200 °C, 1 h), (b) YAG:Ce nanoparticles after LiCl-matrix treatment (600 °C, 1 h) with: size distribution according to SEM (statistical evaluation of >100 nanoparticles), size distribution according to DLS (suspensions in DEG), and SEM images.

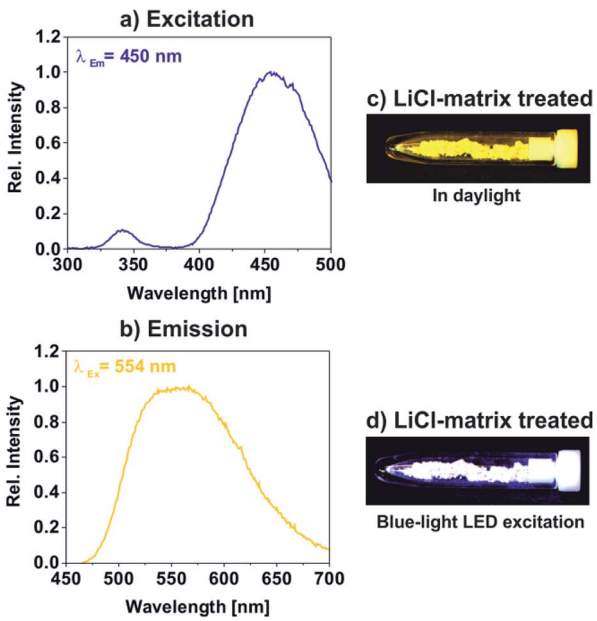

Fig. 6 Excitation (a) and emission (b) spectra of the as-prepared YAG:Ce nanoparticles with powder samples after LiCl-matrix treatment in daylight (c) and with white-light emission under 465 nm excitation of a blue-light LED (d).

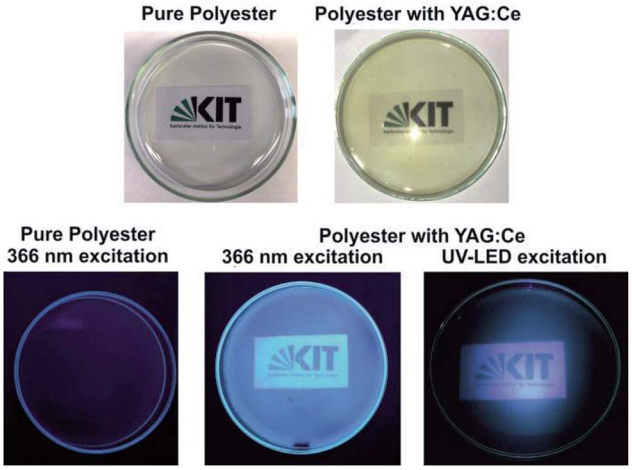

Fig. 7 YAG:Ce nanoparticles after embedding in polyester (2 mg YAG:Ce per 1 g of polyester) in daylight and with 366 nm excitation (Hg discharge lamp) or 405 nm excitation (UV-LED). Pure polyester (without nanoparticles) shown as reference.

LiCl-matrix crystallized YAG:Ce nanoparticles are similar to bulk-YAG:Ce.[1,2] Upon excitation with a blue-light LED lamp, the bright yellow YAG:Ce powder (Fig. 6c) shows intense white light generation due to additive colour mixing of yellow emission of YAG:Ce and reflected blue light of the LED lamp (Fig. 6d). Furthermore, the absolute quantum yield of LiCl-matrix-treated YAG:Ce powder samples was determined following the procedure described by Friend[13] and results in a value of 51(±3)% upon excitation at 454 nm. This value is among the highest quantum yields reported in the literature for YAG:Ce nanoparticles by now.[6b,9a,11]

After the examination of the luminescence properties of YAG:Ce powder samples, embedding the nanoparticles in polymers was tested as a proof-of-the-concept. In this regard, the LiCl-matrix-treated YAG:Ce nanoparticles were again dispersed in a polyol(ethylene glycol). Thereafter, citric acid was added to the suspension, and the polymerization was initiated by heating to 150 °C instantaneously in the liquid phase. The resulting polyester phase contains the YAG:Ce nanoparticles with only 2 mg g^{-1}, resulting in a highly transparent, slightly yellowish polymer (Fig. 7). Upon excitation with a mercury discharge lamp at 366 nm or a UV-LED lamp at 405 nm, the YAG:Ce-containing polyester again shows intense white light generation due to additive colour mixing of yellow emission of YAG:Ce and reflected blue light of the respective light source (Fig. 7). The pure polyester without any nanoparticles as a reference, in contrast, did not show any emission at all (Fig. 7). In sum, the as-prepared YAG:Ce nanoparticles can be used to obtain luminescent and transparent polymers.

Conclusions

In summary, $Y_3Al_5O_{12}:Ce^{3+}$ (YAG:Ce) nanoparticles with a diameter of 30–50 nm were prepared by a two-step approach. This includes microwave-assisted compaction of a pre-formed carbonate precursor in ionic liquids (at 200 °C), followed by LiCl-matrix-treated crystallization (at 600 °C). Mixing of the IL-treated carbonate precursor with LiCl (1 : 10) and heating in the resulting LiCl matrix, on the one hand, allows decomposing the carbonate precursor and crystallizing the YAG phase, and on the other hand, guarantees the separation of the nanoparticles in the LiCl matrix to avoid particle growth and particle agglomeration. Subsequent to the crystallization, the LiCl matrix can be easily removed by rinsing with water, resulting in colloidally stable, dispersible YAG:Ce suspensions.

The YAG:Ce nanoparticles show intense luminescence with a quantum yield of 51(±3)%, which is among the highest values obtained for YAG:Ce nanoparticles. Due to the good dispersibility, the obtained YAG:Ce nanoparticles can be embedded in polymers by polymerization instantaneously in the liquid phase. As a proof-of-the-concept, this is shown for polyester, which shows bright white light emission with only 2 mg YAG:Ce nanoparticles per 1 g of polyester upon excitation with 366 to 465 nm light sources (mercury discharge lamp, UV-LED, blue-light LED) due to additive colour mixing of yellow emission of YAG:Ce and reflected blue light of the respective light source. The presented two-step approach can be optionally transferred to other, high-lattice-energy luminescent materials, such as Y_2O_3:Eu, YVO_4:Eu, $BaMgAl_{10}O_{17}$:Eu, $BaMgAl_{10}O_{17}$:Eu,Mn or Zn_2SiO_4:Mn.

Conflicts of interest

There are no conflicts to declare.

Acknowledgements

The authors acknowledge the Deutsche Forschungsgemeinschaft (DFG) for funding within the priority program SPP1708 “Synthesis near Room Temperature”.

Notes and references

1 S. Ye, F. Xiao, Y. X. Pan, Y. Y. Ma and Q. Y. Zhang, *Mater. Sci. Eng., R*, 2010, **71**, 1.
2 V. Bachmann, C. Ronda and A. Meijerink, *Chem. Mater.*, 2009, **21**, 2077.
3 S. Shionoya, W. M. Yen and H. Yamamoto, *Phosphor Handbook*, CRC Press, Boca Raton, 2006.
4 (*a*) H. K. Yang, H. M. Noh and J. H. Jeong, *Solid State Sci.*, 2014, **27**, 43; (*b*) K. Zhang, W. B. Hu, Y. T. Wu and H. Z. Liu, *Inorg. Mater.*, 2008, **44**, 1218; (*c*) M. Li, D. Zhou, C. P. Li and Z. Zhao, *Mater. Sci. Semicond. Process.*, 2016, **44**, 101; (*d*) L. Gan, Z. Y. Mao, F. F. Xu, Y. C. Zhu and X. J. Liu, *J. Am. Ceram. Soc.*, 2012, **95**, 49.
5 (*a*) M. Borlaf, R. Kubrin, V. Aseev, A. Y. Petrov, N. Nikonorov and T. Graule, *J. Am. Chem. Soc.*, 2017, **100**, 3784; (*b*) A. Boukerika, L. Guerbous and N. Brihi, *J. Alloys Compd.*, 2014, **614**, 383; (*c*) C. Shen, C. Zhong and J. Ming, *J. Exp. Nanosci.*, 2013, **8**, 54; (*d*) S. Mukherjee, V. Sudarsan, R. K. Vatsa and A. K. Tyagi, *J. Lumin.*, 2008, **129**, 69; (*e*) H. M. H. Fadlalla, C. C. Tang, S. Y. Wei and X. X. Ding, *J. Lumin.*, 2008, **128**, 1655; (*f*) B. Masenelli, O. Mollet,

O. Boisron, B. Canut, G. Ledoux, J. M. Bluet, P. Melinon, C. Dujardin and S. Huant, *Nanotechnology*, 2013, **24**, 165703; (*g*) A. Bhaskar, H. Y. Chang, T. H. Chang and S. Y. Cheng, *Mater. Lett.*, 2012, **78**, 124.

6 (*a*) L. Mancic, K. Marinkovic, B. A. Marinkovic, M. Dramicanin and O. Milosevic, *J. Eur. Ceram. Soc.*, 2010, **30**, 577; (*b*) A. Revaux, G. Dantelle, N. George, R. S. Seshadri, T. Gacoin and J. P. Boilot, *Nanoscale*, 2011, **3**, 2015.

7 (*a*) G. Dantelle, D. Testemale, E. Homeyer, A. Cantarano, S. Kodjikian, C. Dujardin, J.-L. Hazemann and A. Ibanez, *RSC Adv.*, 2018, **8**, 26857; (*b*) X. He, X. Liu, R. Li, B. Yang, K. Yu, M. Zeng and R. Yu, *Sci. Rep.*, 2016, **6**, 22238; (*c*) Y. H. Song, G. S. Han, E. K. Ji, M. J. Lee, Y. L. Song, D. S. Kong, M. K. Jung, B. W. Jeong, H. S. Jung and S. H. Yoon, *J. Mater. Chem. C*, 2015, **3**, 6148; (*d*) A. Boukerika, L. Guerbous and N. Brihi, *J. Alloys Compd.*, 2014, **614**, 383; (*e*) A. Aboulaich, J. Deschamps, R. Deloncle, A. Potdevin, B. Devouard, G. Chadeyron and R. Mahiou, *New J. Chem.*, 2012, **36**, 2493; (*f*) X. Zhou, K. Zhou, Y. Li, Z. Wang and Q. Feng, *J. Lumin.*, 2012, **132**, 3004; (*g*) H. J. Byun, W. S. Song, Y. S. Kim and H. Yang, *J. Phys. D*, 2010, **43**, 195401.

8 (*a*) M. Odziomek, F. Chaput, F. Lerouge, M. Sitarz and S. Parola, *J. Mater. Chem. C*, 2017, **5**, 12561; (*b*) H. Yang and Y. S. Kim, *J. Lumin.*, 2008, **128**, 1570.

9 (*a*) L. Song, Y. Dong, Q. Shao and J. Jiang, *J. Mater. Sci.*, 2018, **53**, 15196; (*b*) J. D. Furman, G. Gundiah, K. Page, N. Pizarro and A. K. Cheetham, *Chem. Phys. Lett.*, 2008, **465**, 67.

10 (*a*) W. Shi, A. Feng, H. Tang, Z. Ding, Y. Ma, M. Wu and G. Li, *Opt. Mater.*, 2013, **35**, 609; (*b*) K. Zhang, W. Hu, Y. Wu and H. Liu, *Ceram. Int.*, 2009, **35**, 719; (*c*) V. Pankratov, L. Grigorjeva, D. Millers and T. Chudoba, *Radiat. Meas.*, 2007, **42**, 679.

11 A. Revaux, G. Dantelle, D. Decanini, A. M. Haghri-Gosnet, T. Gacoin and J. P. Boilot, *Opt. Mater.*, 2011, **33**, 1124.

12 T. Welton, *Chem. Rev.*, 1999, **99**, 2071.

13 J. C. de Mello, H. F. Wittmann and R. H. Friend, *Adv. Mater.*, 1997, **9**, 230.

14 (*a*) M. Baghbanzadeh, L. Carbone, P. D. Cozzoli and C. O. Kappe, *Angew. Chem., Int. Ed.*, 2011, **50**, 11312; (*b*) M. Antonietti, D. Kuang, B. Smarsly and Y. Zhou, *Angew. Chem., Int. Ed.*, 2004, **43**, 4989.

15 (*a*) G. Bühler and C. Feldmann, *Angew. Chem., Int. Ed.*, 2006, **45**, 4864; (*b*) P. Wasserscheid and T. Welton, *Ionic Liquids in Synthesis*, Wiley-VCH, Weinheim, 2008.

16 H. Dong, Y. C. Chen and C. Feldmann, *Green Chem.*, 2015, **17**, 4107.

17 M. S. Ata, Y. Liu and I. Zhitomirsky, *RSC Adv.*, 2014, **4**, 22716.

18 D. C. Harris and C. A. Lucy, *Quantitative Chemical Analysis*, Freeman Publishers, New York, 9th edn, 2016, p. 529.